

THE PSEUDOSPARK AS AN ELECTRON BEAM SOURCE*

E. Boggasch, T.A. Fine, M.J. Rhee
Laboratory for Plasma Research
University of Maryland, College Park, MD 20742

Abstract

The pseudospark is a low pressure, hollow-cathode gas discharge that occurs in a special discharge geometry (pseudospark chamber) in different kinds of gases. A modular pseudospark chamber was built to investigate this new discharge type as a source of intense electron beams. At a breakdown voltage of 24 kV and a discharge current of 480 A, an electron beam of 106 A and 13 ns FWHM was extracted through the anode hole into a drift chamber filled with low pressure gas. Electrical parameters of the circuit, including the plasma channel, were evaluated by monitoring the discharge current waveform. First results of beam profile and emittance measurements of the produced electron beam are presented. At an axial distance of 9 cm behind the anode an rms emittance of 55 mm-mrad was measured.

Introduction

The "pseudospark" phenomenon was first reported by Christiansen and Schultheiss in 1978¹ as a fast, low pressure gas discharge which occurred in a special device, called a pseudospark chamber. The formation time of this discharge is similar to that of a high pressure spark; its mechanisms, however, appear to be totally different.² A single gap pseudospark chamber consists of an anode with a center hole and a hollow-cathode, both electrodes separated by an insulating washer of a few mm width. The voltage holdoff capability of such a single gap pseudospark structure depends on the gap width and the gas pressure inside the chamber. A characteristic breakdown curve for such a structure (breakdown voltage vs. pressure times distance) similar to the Paschen curve for parallel electrodes is obtained. The pseudospark is initiated on the left side of this breakdown curve. In this region, a gas discharge occurs along the longest possible discharge path which, in the case of a pseudospark geometry, is defined on the axis. The holdoff capability of one gap is limited to 40 to 50 kV due to onset of surface flashover and field emission. This holdoff voltage is enhanced by additional stacks of intermediate electrode and insulator discs forming a multigap chamber. Statically, the voltage is capacitively divided, reducing the voltage across one gap by the number of stacks. Multigap chambers are also reported to produce intense pulsed electron beams of up to 1 kA current, 10^9 W/cm² power, and typically 20 ns pulse length.³

Experiment

An easy to change, o-ring sealed, modular discharge chamber system with brass electrodes and plexiglas discs was designed. For the experiments reported here a 6 gap pseudospark chamber with a 3 mm diam center hole on axis was used. The experimental setup is shown in Fig. 1. Negative high-voltage up to 35 kV is applied to the hollow-cathode via a 200 M Ω current limiting resistor. In addition to the self-capacitance of 11 pF of the chamber, the total capacitance was increased by adding external capacitors of up to 760 pF to investigate the discharge characteristics for different stored energies. The chamber was mounted on a plexiglas drift tube of 50 cm length and 6.3 cm diameter. A brass flange which terminated the tube was connected via 6 brass bars equally spaced on a radius of 44 mm to the grounded anode, thus providing a current return path.

A two-stage mechanical pump evacuated the assembly to about 1 mTorr. The working gas was usually argon which was injected through a needle valve from the cathode side into the system. The operating pressure range varied from 20 to 60 mTorr.

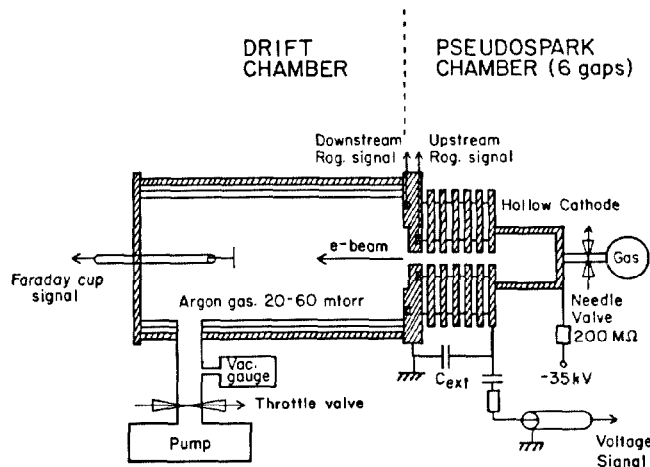


Fig. 1. Experimental set up.

Two calibrated miniature Rogowski coils surrounding the center hole were built into the anode flange as can be seen in Fig. 1. The coil facing the cathode side (upstream coil) measured the total current in the discharge channel. The other coil facing the drift chamber (downstream coil) measured the current which passed through the anode hole into the drift chamber. The chamber voltage was measured by a capacitively coupled resistive voltage probe of division ratio 1:20000 in a 50 Ω load. It was connected via a 1.4 pF capacitor to the cathode. The risetime of this probe after proper compensation is less than 400 ps and its RC decay constant is 116 ns.

A movable 1 m Ω graphite Faraday cup of 3 cm diam was inserted on axis through the end flange of the drift tube to measure the electron beam current at certain distances downstream of the anode.

The emittance of the electron beam was analyzed using a slit-hole type emittance meter.⁴ It consisted of an array of seven 2 mm separated slits of 200 μ m width which were cut into a 0.6 mm thick stainless steel plate. These slits produce sheet beamlets which are detected by a special radiachromic film⁵ placed 12 mm further downstream. The film material gives linear coloration response up to an absorbed dose of 10^8 rad. By use of an applied magnetic field, it was proved that UV or other light did not contribute to the film response. The resulting spatial pattern distribution on the film was scanned by a microdensitometer from which the emittance and beam profile can be found.⁴

The low pressure breakdown characteristic of the discharge chamber was determined by fixing the voltage to a certain value and slowly increasing the pressure until breakdown occurred. In Fig. 2 the breakdown voltage U_B is plotted as a function of pressure. With decreasing pressure, U_B is increasing.

When the power supply with voltage U_0 is connected via a resistor R , the chamber capacitance C is charged up. At a certain pressure and voltage, defined by the characteristic breakdown curve (Fig. 2), the voltage breaks down. The charging resistor R decouples the discharge plasma from the current source and limits the current. Therefore the low impedance discharge cannot be sustained, and is extinguished. Consequently the voltage across the chamber capacitance C rises again until the breakdown voltage U_B is reached and the cycle can start again. Thus a periodic, pulsed discharge is obtained, the frequency f of which is approximately determined by

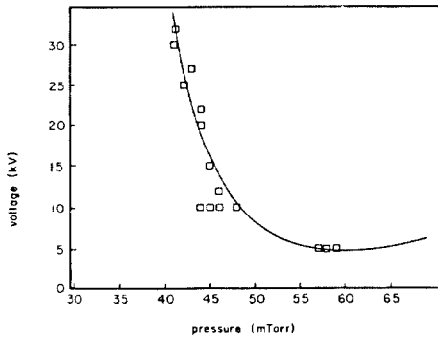


Fig. 2. Characteristic breakdown curve.

$$f = \left[RC \ln \frac{U_0}{U_0 - U_B} \right]^{-1} \quad (1)$$

By choosing the RC value adequately a frequency of typically a few HZ can be obtained.

Results

Fig. 3 shows a typical set of electrical signals obtained by Rogowski coils, voltage probe and Faraday cup, all triggered by the same voltage signal. The discharge current is measured by the upstream Rogowski coil and shows a damped oscillating waveform. The voltage drops within 20 ns from 90% to 10%. The maximum current corresponds to almost zero voltage indicating the mainly inductive behavior of the discharge. The downstream coil, as well as the Faraday cup register one negative peak at the time of the discharge current maximum.

All signals show that the breakdown process occurs in two stages. Up to time t_p the voltage drops slowly, and upstream and downstream current start smoothly. At time t_p the main discharge occurs. This two-step breakdown is also visible in the waveform of the downstream Faraday cup signal. Of 106 A electron current leaving the anode, as registered by the downstream Rogowski coil, only 40 A are measured by the Faraday cup, 15 cm downstream of the anode.

The discharge current waveform was fitted for two different external capacitor values C using the expression

$$I(t) = I(0) \exp\left(\frac{R(t-t_0)}{2L}\right) \sin[\omega(t-t_0)], \quad (2)$$

$$\text{where } \omega = \left[\frac{1}{LC} - \left(\frac{R}{2L}\right)^2 \right]^{1/2}.$$

Thus, time average values for the discharge inductance L and the resistance R could be determined, as is summarized in Table I.

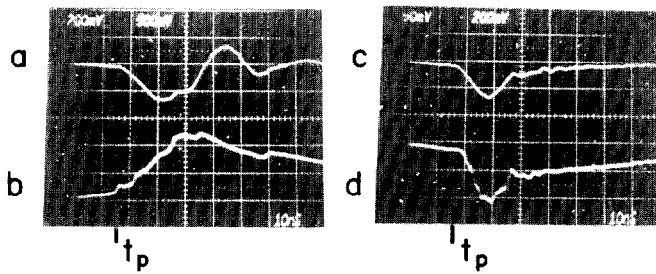


Fig. 3. Typical electrical signals of discharge. a) discharge current (upstream coil) 360 A/div; b) voltage signal 10 kV/div; c) injected electron beam current (downstream coil) 84 A/div; d) Faraday cup signal (15 cm behind anode) 20 A/div.

Table I.
Inductance L and resistance R for different discharge conditions calculated according to (2).

C(pF)	20 kV		25 kV		30 kV	
	R(Ω)	L(nH)	R(Ω)	L(nH)	R(Ω)	L(nH)
420	2.2	56.2	2.1	57.5	1.7	55.3
760	1.7	40.9	1.9	40.2	1.8	44.4

The dependence of discharge current and beam current as measured by the upstream and downstream coil as a function of charging voltage for two capacitance values is illustrated in Fig. 4. Both current signals show an increase in amplitude with increasing voltage and capacitance. For the following measurements of beam radius and emittance an external capacitance of 390 pF was added to the chamber, the breakdown voltage was 24 kV. These results were obtained by averaging more than 20 shots.

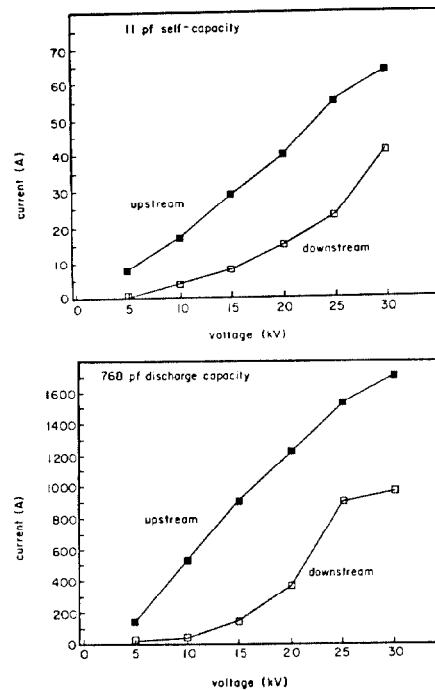


Fig. 4. Upstream and downstream coil current as a function of charging voltage for discharge capacity values.

To find the beam radius at different axial distances from the anode, the experimental data was fitted to a Gaussian profile. The values for the least square fit rms radius b are shown in Fig. 5. The beam expands from an rms radius of 1.5 mm at 30 mm distance to 2.5 mm radius at 180 mm distance behind the anode as it propagates through the low pressure gas.

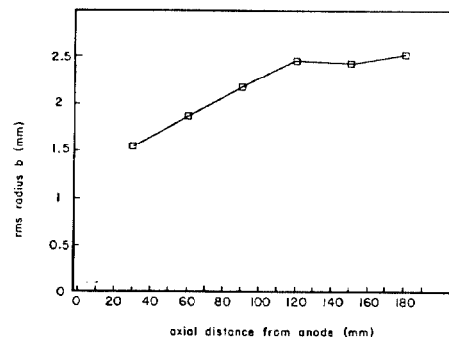


Fig. 5. RMS radius b as function of distance from anode.

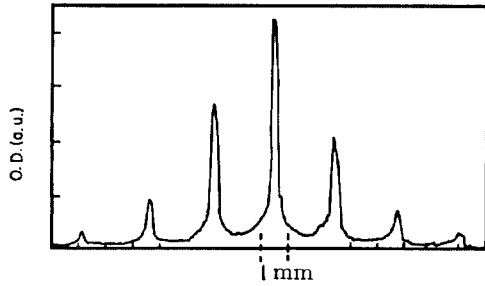


Fig. 6. Density distribution (optical density O.D.) found behind a 7 slit system in a 9 cm distance from anode.

Fig. 6 shows the scanned beamlet distribution profile at 9 cm downstream of the anode. By careful data evaluation a three dimensional emittance plot is obtained (Fig. 7). The rms emittance, $\bar{\epsilon}$, assuming a Maxwellian transverse velocity distribution and Gaussian density profile, is calculated by numerical integration⁴ and found to be

$$\bar{\epsilon} = 55 \text{ mm} - \text{mrad}$$

For this case the rms radius $b = 2.18 \text{ mm}$ and a constant rms width σ of 6 mrad was used. The latter value was measured with a $60 \mu\text{m}$ knife edge shaped slit. For an estimated mean beam energy of 20 keV, this leads to a normalized rms emittance $\bar{\epsilon}_n$ of 14.76 mm-mrad.

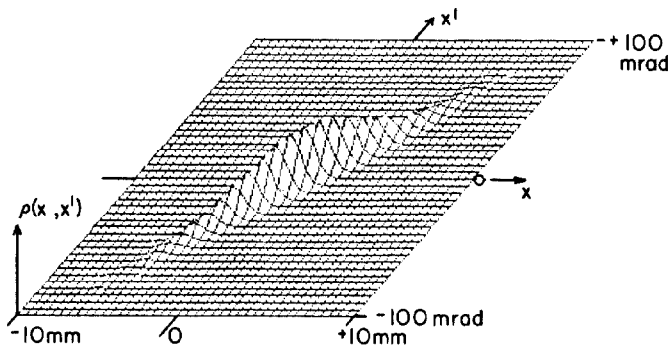


Fig. 7. Three-dimensional phase space density contour plot $\rho(x, x')$

Conclusions

The electrical characteristics of a pseudospark discharge and the emittance of the ejected electron beam in argon gas have been investigated.

The pseudospark discharge occurs rather reproducibly at the pressure and voltage defined by the characteristic breakdown curve. The breakdown takes place in two stages, each of which is accompanied by electron beam emission. The electron energy distribution has still to be determined. After the electron emission occurs, the discharge drops into a low impedance mode whose waveform was modeled, assuming a simple LRC circuit analysis. The electron beam propagates, self-focused, in low pressure gas. The time integrated emittance was measured at an axial distance of 9 cm behind the anode. An rms value of about 55 mm-mrad was found. Together with the measured beam current I of 50 A at that distance and the normalized rms emittance $\bar{\epsilon}_n \approx 15 \text{ mm-mrad}$, an intrinsic normalized brightness B_n of about

$$B_n = \frac{I}{(\bar{\epsilon}_n)^2} \approx 2 \cdot 10^{11} \frac{\text{A}}{\text{m}^2 \text{ rad}^2}$$

is obtained. This classifies the pseudospark discharge as a high brightness electron beam source.

Acknowledgments

We would like to acknowledge the technical assistance of D. Cohen and C. Daniels. This work is supported by the Air Force Office of Scientific Research and the U.S. Department of Energy.

References

1. J. Christiansen, Ch. Schultheiss, Z. Phys. **A290**, 35 (1979).
2. K. Frank, J. Christiansen, Proc. 13th Int'l. Sym. on Discharges and Electrical Insulation in Vacuum, Vol. 2, Paris, June 27-30, 1988.
3. W. Benker, J. Christiansen, K. Frank, H. Gundel, W. Harman, A. Niederlöhner, T. Redel, M. Stetter, Proc. 13th Int'l. Sym. on Discharges and Electrical Insulation in Vacuum, Vol. 2, Paris, June 27-30, 1988.
4. M.J. Rhee and R.F. Schneider, Part. Accel. **20**, 133 (1986).
5. W.L. McLaughlin, R.M. Uribe, and A. Miller, Radiat. Phys. Chem. **22**, 333 (1983).